American Mineralogist, Volume 70, pages 249–260, 1985

Low-temperature heat capacities and derived thermodynamic properties of anthophyllite, diopside, enstatite, bronzite, and wollastonite

KENNETH M. KRUPKA[1]

Department of Geosciences
The Pennsylvania State University
University Park, Pennsylvania 16802

RICHARD A. ROBIE, BRUCE S. HEMINGWAY

U.S. Geological Survey
Reston, Virginia 22092

DERRILL M. KERRICK

Department of Geosciences
The Pennsylvania State University
University Park, Pennsylvania 16802

AND JUN ITO[2]

The James Franck Institute
The University of Chicago
Chicago, Illinois 60637

Abstract

The heat capacities for magnesio-anthophyllite, diopside, synthetic enstatite, bronzite, and wollastonite were measured between 5 and 385 K by use of an adiabatic calorimeter. The entropy change $S^\circ_{298} - S^\circ_0$, in J/(mol·K), is 538.9 ± 2.7 for magnesio-anthophyllite [$Mg_{6.3}Fe_{0.7}Si_8O_{22}(OH)_2$], 142.7 ± 0.2 for diopside, 66.27 ± 0.10 for synthetic enstatite ($MgSiO_3$), 69.04 ± 0.10 for bronzite ($Mg_{0.85}Fe_{0.15}SiO_3$), and 81.69 ± 0.12 for wollastonite. The heat capacity, C°_P, for magnesio-anthophyllite, corrected to a composition of pure Mg-anthophyllite [$Mg_7Si_8O_{22}(OH)_2$], results in a $S^\circ_{298} - S^\circ_0$ value of 537.0 ± 2.7 J/(mol·K). These results represent only the entropy calculated from the measured heat capacities. No configurational entropy was added.

Although our C°_P values for diopside and wollastonite differ significantly from those of previous studies, especially at cryogenic temperatures, our entropies at 298.15 K are in close agreement with the commonly accepted values. Schottky heat capacity anomalies were observed below 25 K for magnesio-anthophyllite, diopside, and bronzite. The contribution of the magnetic entropy arising from the interaction of Fe^{2+} with the ligand field of the crystals is discussed.

Introduction

The previously accepted entropies for diopside and wollastonite at 298.15 K were based on a limited number of low-temperature C°_P measurements. King (1957) and Wagner (1932) reported C°_P values for diopside between 50 and 300 K and between 20 and 40 K, respectively. Wagner (1932) also measured the C°_P of wollastonite over several, often narrow, temperature intervals between 9 and 304 K. Prior to this study, low-temperature C°_P data for magnesio-anthophyllite and enstatite were nonexistent, and heat capacity measurements by Kelley (1943) between 52 and 296 K for a poorly characterized sample of clinoenstatite were used to estimate the thermodynamic properties of enstatite. Reliable values for the entropies of these phases are critically important to calculating the high-temperature stability of these minerals and the metamorphic and igneous equilibria involving them.

[1] Present address: Geosciences Research and Engineering Department, Battelle, Pacific Northwest Laboratories, Richland, Washington 99352.

[2] Deceased.

0003–004X/85/0304–0249$02.00

Table 1. Chemical analyses of samples used in low-temperature heat capacity measurements

	Magnesio-anthophyllite[a]	Diopside[a]	Enstatite (synthetic)[b]	Bronzite (natural)[c]	Wollastonite[a]
SiO_2	59.4	55.3	59.28	55.86	51.8
TiO_2	0.1	0.00	---	---	0.00
Al_2O_3	0.95	0.20	0.00	0.66	<0.05
Cr_2O_3	0.11	---	---	0.10	---
Fe_2O_3	0.57	0.09	---	---	0.05[d]
FeO	5.7	0.48	0.12[e]	10.11[e]	---
MgO	30.2	18.0	40.80	31.61	0.12
MnO	0.12	0.04	---	0.19	0.00
NiO	0.12	---	---	---	---
CaO	0.62	25.2	0.00	0.29	48.5
Na_2O	0.20	0.01	---	---	0.01
K_2O	0.07	0.02	---	---	0.01
P_2O_5	0.03	0.03	---	---	0.00
CO_2	0.01	0.01	---	---	0.00
H_2O^+	2.1	0.64	---	---	<0.01
H_2O-	0.22	0.08	---	---	---
Total:	100.52	100.10	100.20	98.82	100.49

[a]Analyses completed by combination of atomic absorption spectroscopy and standard wet-chemical techniques. See Shapiro (1975) for a description of these analytical techniques.
[b]Average of 84 spot probe analyses.
[c]Weighted average of a total of 55 spot probe analyses for 31 bronzite chips.
[d]Total iron as Fe_2O_3.
[e]Total iron as FeO.

Minerals

Magnesio-anthophyllite, $Mg_{6.3}Fe_{0.7}Si_8O_{22}(OH)_2$

The anthophyllite sample, designated 7.3.71.10, was collected by Prof. Peter Misch in the North Cascades at mile-marker 132.5 along the North Cascades Highway (Washington Route 20) north of the eastern part of Lake Diablo. A small vein of light-green, coarse-bladed anthophyllite was cut from the specimen, crushed, and sieved to the range of −35 to +100 mesh. Impurities were removed from the sample by using a Franz[3] magnetic separator and heavy-liquid techniques. X-ray powder-diffraction methods showed that the separated anthophyllite contained talc (< 5%) as the only impurity.

The chemical analysis given in Table 1 is in close agreement with unpublished electron probe analyses provided by Prof. Misch and with other probe analyses completed during this study. Orthorhombic symmetry for the sample was confirmed by use of a petrographic microscope. The unit-cell dimensions for the calorimetric sample, given in Table 2, are in good agreement with the values for synthetic, pure-Mg anthophyllite (Chernosky and Autio, 1979) and for natural anthophyllite (Finger, 1970).

The anthophyllite sample was also analyzed for the presence of hydrous pyribole structures (Veblen et al., 1977; Veblen and Burnham, 1978a,b). The magnesio-anthophyllite sample is composed of at least 95 percent (by volume) double chain material and approximately 5 percent wider chains (Veblen, written communication, 1978). The distribution of disordered, wider chain material is not homogeneous in the sample. A description of the intergrowth structures in this anthophyllite sample was given by Veblen and Buseck (1979).

Diopside, $CaMg(SiO_3)_2$

The white diopside sample was collected by one of us (DMK) from an area near Zermatt, Switzerland studied by Bearth (1970), and was used in the experimental study of Slaughter et al. (1975). Examinations by means of X-ray diffraction and a petrographic microscope did not reveal any impurities in the powdered diopside. The chemical composition given in Table 1 is in close agreement with the analyses presented by Slaughter et al. (1975). The cell dimensions given in Table 2 are in excellent agreement with the values for diopside presented by Borg and Smith (1969) and in the Joint Committee of Powder Diffraction Standards (JCPDS) file 11-654.

Bronzite, $Mg_{0.85}Fe_{0.15}SiO_3$

The bronzite sample was described by Huebner et al. (1979). The calorimetric sample consisted of 31 pale-brown, single-crystal chips, that ranged in mass from 0.19 to 1.65 g. Optical examination of each chip did not reveal any impurities. The composition of each chip was determined by electron-microprobe analysis using the method of Bence and Albee (1968). Multiple spot analyses of each chip revealed no chemical inhomogeneities within any single chip. A weighted-average chemical composition for this sample is given in Table 1. Unit-cell dimensions were measured for the most Mg- and Fe-rich bronzite chips, designated K30 and K31, respectively. The refined cell constants (Table 2) are in good agreement with those for bronzite as given in JCPDS patterns 19-605 and 26-876.

Synthetic enstatite, $MgSiO_3$

Enstatite crystals were prepared by growth from a lithium-vanadomolybdate flux using the method of Ito (1975). Residual flux was removed by solution with H_2O in a sonic cleaner after gentle crushing of the crystals. Further details are given by Krupka (1984). Semi-quantitative emission spectroscopy analysis detected (maximal values): Li = 1100 ppm, Mo = 1200 ppm, Ni = 100 ppm, P = 910 ppm, V = 1500 ppm, and Zr = 120 ppm. Microprobe results (Table 1) show that the synthetic enstatite is essentially pure, stoichiometric $MgSiO_3$. Unit-cell dimensions were measured for two samples of synthetic $MgSiO_3$ and are given in Table 2. Cell dimensions of the calorimetric sample are in excellent agreement with those given by Ito (1975) for a similarly synthesized enstatite.

Wollastonite, $CaSiO_3$

The wollastonite sample from Willsboro, Essex County, New York, was purchased from Wards Natural Science Establishment. The specimen was crushed, sieved to the range of −35 to +100 mesh, and separated by heavy-liquid techniques. X-ray diffraction and optical measurements on the final sample did not reveal any impurities. Chemical analyses of the separated wollastonite are given in Table 1. The refined cell constants (Table 2) are in close agreement with the values for wollastonite given by Buerger and Prewitt (1961).

[3] The use of trade names is for descriptive purposes only and does not imply endorsement by Battelle, Pacific Northwest Laboratories, U.S. Geologic Survey, or The Pennsylvania State University.

Table 2. Cell constants for samples used in heat capacity measurements

	Magnesio-anthophyllite	Diopside	Bronzite (natural) K30	Bronzite (natural) K31	Enstatite (synthetic) Ito-1	Enstatite (synthetic) Ito-7	Wollastonite
a (nm)	1.8536(3)	0.9749(1)	1.8250(3)	1.8249(2)	1.8228(2)	1.8219(2)	0.7925(1)
b (nm)	1.7999(3)	0.8925(1)	0.8837(1)	0.8843(1)	0.8816(1)	0.8814(1)	0.7322(2)
c (nm)	0.5277(1)	0.52511(9)	0.5190(1)	0.5193(1)	0.5180(1)	0.5178(1)	0.7069(1)
α	90°	90°	90°	90°	90°	90°	90° 4'(2)
β	90°	105° 48.2'(9)	90°	90°	90°	90°	95° 13.8'(9)
γ	90°	90°	90°	90°	90°	90°	103° 19'(1)
V (nm^3)	1.7606(4)	0.43966(8)	0.8370(2)	0.8380(2)	0.8325(2)	0.8316(2)	0.3974(1)
N	38	32	29	30	28	34	23

Note: Cell dimensions given in nanometers (1 nm = 10 Å). Number in parentheses is uncertainty in last digit. Cell dimensions were measured using CuKα radiation, a Ni filter, a scanning rate of 0.25° 2θ/min, and BaF_2 (a = 0.61971 ± 0.0001 nm) as an internal standard.
N = Number of reflections used in least-squares refinement program written by Appleman and Evans (1973).

Apparatus and procedures

Low-temperature C_P° measurements were made using the apparatus and techniques described by Robie and Hemingway (1972) and Robie et al. (1976). The observed heat capacities were corrected for curvature (Robie and Hemingway, 1972) and for small quantities of He gas, generally between 9.6×10^{-5} and 8.4×10^{-4} moles of gas, which were introduced into the calorimeter during the loading in order to promote thermal equilibration at cryogenic temperatures (Robie et al., 1976). The 1975 atomic weights (Commission on Atomic Weights, 1976), were used to calculate the gram-formula weights of the measured compounds.

Experimental results

The experimental specific heats of magnesio-anthophyllite, diopside, bronzite, synthetic enstatite, and wollastonite are listed in their chronological order of measurement in Tables 3 through 7, respectively. The sample masses (in vacuo) and number of calorimetric measurements made with each sample are given in the headings of Table 3 through 7. These experimental values have been corrected for curvature but not for deviation from their ideal end-member formulas. The estimated uncertainty of the experimental data is ±5.0% at 5 K, ±1.0% at 15 K, and ±0.15% between 25 and 380 K (Robie et al., 1978). The experimental C_P° data, corrected for impurities, are shown in Figures 1 through 4.

The experimental C_P° data for magnesio-anthophyllite were corrected for chemical impurities (secondary phases) and for deviation from end-member stoichiometry by the procedure described by Krupka (1984) and Robie et al. (1976, p. 640). Corrections were first applied to the C_P° data to obtain a solid-solution magnesio-anthophyllite [$Mg_{6.3}Fe_{0.7}Si_8O_{22}(OH)_2$] by assuming that 848.382 g of impure anthophyllite consist of 1 mole of magnesio-anthophyllite (802.900 g) and 14.239 g $NaAlSi_3O_8$ glass, 10.838 g $CaSiO_3$ (wollastonite), 5.711 g Fe_2O_3 (hematite), 4.629 g Al_2O_3 (corundum), 4.350 g SiO_2 (quartz), 3.535 g $KAlSi_3O_8$ glass, 2.552 g $Fe_{0.8}S$ (pyrrhotite), and 1.022 g MnO (manganosite). The low-temperature C_P° data for $NaAlSi_3O_8$ and $KAlSi_3O_8$ glasses were from Robie et al. (1978), $CaSiO_3$ from this study, Fe_2O_3 from Gronvold and Westrum (1959), Al_2O_3 from Furukawa et al. (1956), SiO_2 from unpublished data by Prof. E. F. Westrum, Jr. (University of Michigan), $Fe_{0.8}S$ from Gronvold et al. (1959), amosite from Bennington et al. (1978), and the remainder of the C_P° data were taken from Kelley and King (1961). The selection of these phases for impurity corrections was based on the availability of accurate C_P° data for the constituents. The difference between the uncorrected C_P° values and those calculated for $Mg_{6.3}Fe_{0.7}Si_8O_{22}(OH)_2$ is 3.8% at 50 K, and ≤0.5% at all temperatures greater than 100 K.

The experimental C_P° data for magnesio-anthophyllite were similarly corrected to a pure Mg-anthophyllite by assuming that 936.445 g of the impure sample contains 1 mole of Mg-anthophyllite [$Mg_7Si_8O_{22}(OH)_2$, 780.874 g], and 103.982 g $Fe_7Si_8O_{22}(OH)_2$ (amosite-fibrous ferro-anthophyllite), 15.734 g $NaAlSi_3O_8$ glass, 11.977 g $CaSiO_3$ (wollastonite), 6.306 g Fe_2O_3 (hematite), 5.108 g Al_2O_3 (corundum), 4.771 g SiO_2 (quartz), 3.924 g $KAlSi_3O_8$ glass, 2.815 g $FeO_{0.8}S$ (pyrrhotite), and 1.128 g MnO (manganosite). The difference between the uncorrected and corrected C_P° values is 14% at 50 K, decreases to 0.3% at 100 K, and increases to approximately 3% at temperatures greater than 275 K.

The C_P° data for diopside were corrected for chemical

Table 3. Low-temperature, experimental specific heats of magnesio-anthophyllite. (Sample mass was 22.111 g (in vacuo). Data for magnesio-anthophyllite consist of 94 measurements between 5.4 and 386.0 K.)

Temp. K	Specific heat J/(g·K)	Temp. K	Specific heat J/(g·K)	Temp. K	Specific heat J/(g·K)
Series 1		Series 4		Series 7	
305.29	0.8379	140.17	0.4013	5.43	0.001148
311.12	0.8476	145.11	0.4195	6.00	0.001523
317.34	0.8584	150.13	0.4376	6.61	0.001907
323.41	0.8685	155.18	0.4552	7.35	0.002399
329.43	0.8782	160.22	0.4727	8.21	0.002922
335.40	0.8882	165.26	0.4897	9.07	0.003410
		170.30	0.5064	9.95	0.003911
Series 2		175.35	0.5228	10.97	0.004462
		180.41	0.5392	12.13	0.004998
341.71	0.8981	185.48	0.5547	13.38	0.005430
347.70	0.9069	190.57	0.5702	14.72	0.005880
353.66	0.9159	195.68	0.5852	16.19	0.006361
359.57	0.9242	200.81	0.6000	17.79	0.007015
365.40	0.9331			19.54	0.007979
371.10	0.9413	Series 5		21.46	0.009164
376.97	0.9490			23.53	0.01070
382.08	0.9553	205.94	0.6144	25.81	0.01275
385.99	0.9597	211.00	0.6285	28.32	0.01552
		215.93	0.6416	31.06	0.01922
Series 3		220.90	0.6548	34.25	0.02444
		225.91	0.6677	37.66	0.03084
51.10	0.06693	230.87	0.6801	41.25	0.03839
56.15	0.07931	235.87	0.6928	45.30	0.04783
60.76	0.09406	240.90	0.7051		
65.60	0.1102	245.89	0.7168	Series 8	
70.53	0.1278	250.83	0.7280		
75.70	0.1472	255.81	0.7390	50.42	0.06145
81.00	0.1679			54.86	0.07483
86.10	0.1883	Series 6		59.67	0.08989
91.05	0.2081				
95.78	0.2270	260.84	0.7500		
100.48	0.2459	265.84	0.7610		
105.42	0.2656	270.88	0.7717		
110.36	0.2855	275.97	0.7820		
115.32	0.3053	281.02	0.7923		
120.32	0.3253	286.04	0.8025		
125.35	0.3450	291.10	0.8131		
130.33	0.3643	296.22	0.8217		
135.15	0.3825	301.31	0.8310		
		306.45	0.8403		
		311.65	0.8489		

impurities and for deviation from end-member stoichiometry by the same procedure used for anthophyllite. A sample of 222.321 g was assumed to consist of 1 mole of diopside [$CaMg(SiO_3)_2$, 216.553 g] and 3.617 g SiO_2 (quartz), 1.381 g Fe_2O_3 (hematite), 0.444 g Al_2O_3 (corundum), 0.348 g CaO, and 0.092 g MnO (manganosite). The difference between the uncorrected and corrected C_p° values is 3.3% at 20 K, 0.9% at 50 K, and approximately 0.15% at all temperatures greater than 100 K.

The experimental C_p° data for wollastonite were corrected for impurities and deviation from end-member stoichiometry by assuming that a 116.604 g of sample consists of 1 mole of pure wollastonite ($CaSiO_3$, 116.164 g) and 0.185 g CaO, 0.141 g MgO (periclase), 0.061 g Al_2O_3 (corundum), and 0.056 g Fe_2O_3 (hematite). The difference between the uncorrected and impurity-corrected C_p° values is 0.25% at 20 K, 0.08% at 100 K, and less than 0.03% at all temperatures greater than 150 K.

Below 25 K, the specific heats for magnesio-anthophyllite, diopside, and bronzite are significantly larger than those for wollastonite and synthetic enstatite. This difference is presumably due to a Schottky-type contribution (Gopal, 1966) to the heat capacity at very low temperatures arising from the small amount of Fe^{2+} in solid solution. Because the Schottky contributions are significant for the magnesio-anthophyllite and bronzite samples, their heat capacities exhibit anomalous "plateaus" near 15 K. The C_p° anomalies are especially apparent when the data are plotted in the form of C_p°/T versus T^2, where the anomalies are seen to have a maximum value near 100 K^2 (Fig. 5). The evaluation of the entropy contribution from the Schottky effects for bronzite will be discussed in a later section.

Table 4. Low-temperature, experimental specific heats of diopside. (Sample mass was 32.083 g (in vacuo). Data for diopside consist of 92 measurements between 8.6 and 382.0 K.)

Temp. K	Specific heat J/(g·K)	Temp. K	Specific heat J/(g·K)	Temp. K	Specific heat J/(g·K)
Series 1		Series 5		Series 9	
298.38	0.7692	107.87	0.2728	237.52	0.6577
302.64	0.7765	112.82	0.2919	243.69	0.6706
308.20	0.7848	117.67	0.3104	249.79	0.6829
314.55	0.7946	123.61	0.3326	255.81	0.6944
321.52	0.8047	129.67	0.3548	261.77	0.7062
328.24	0.8141	134.88	0.3735	267.67	0.7174
334.91	0.8233	140.28	0.3923	273.54	0.7283
341.53	0.8319	145.80	0.4110	279.39	0.7378
				285.19	0.7475
Series 2		Series 6			
				Series 10	
336.38	0.8252	151.36	0.4294		
343.10	0.8339	156.90	0.4472	8.62	0.001184
		162.36	0.4643	9.32	0.001311
Series 3		167.68	0.4806	9.97	0.001442
		172.90	0.4961		
349.68	0.8426	178.01	0.5110	Series 11	
356.23	0.8509	183.05	0.5251		
362.73	0.8591	188.05	0.5391	11.35	0.001578
369.19	0.8669	193.04	0.5523	12.26	0.001591
375.61	0.8747	198.04	0.5653	13.40	0.001818
381.99	0.8815	203.09	0.5781	14.72	0.002072
		208.24	0.5908	16.19	0.002388
Series 4		213.51	0.6033	17.78	0.002864
		218.92	0.6161	19.47	0.003602
54.74	0.07265	224.49	0.6288	21.37	0.004638
60.50	0.09142			23.56	0.006166
65.44	0.1084	Series 7		25.93	0.008311
70.33	0.1261			28.53	0.01125
75.36	0.1451	229.78	0.6407	31.33	0.01520
80.41	0.1647	235.79	0.6539	34.34	0.02036
85.52	0.1850	241.93	0.6669	37.69	0.02695
90.66	0.2053	248.27	0.6835	41.45	0.03527
95.81	0.2256	254.82	0.6937	45.64	0.04568
100.94	0.2458	261.51	0.7076	50.24	0.05854
				55.29	0.07421
		Series 8		60.66	0.09176
		268.15	0.7250		
		274.93	0.7312		
		281.63	0.7422		
		288.22	0.7538		
		294.64	0.7640		
		300.87	0.7737		

Table 5. Low-temperature, experimental specific heats of bronzite. (Sample mass was 25.762 g (in vacuo). Data for bronzite consist of 96 measurements between 5.5 and 387.4 K.)

Temp. K	Specific heat J/(g·K)	Temp. K	Specific heat J/(g·K)	Temp. K	Specific heat J/(g·K)
Series 1		Series 6		Series 10	
297.37	0.7728	121.71	0.3137	288.41	0.7599
300.74	0.7809	126.62	0.3321	293.79	0.7701
306.43	0.7908	131.55	0.3503	299.23	0.7787
312.40	0.8004	136.61	0.3685	304.64	0.7873
318.43	0.8098	141.69	0.3864		
324.60	0.8193			Series 11	
330.80	0.8282	Series 7			
336.89	0.8374			5.50	0.002114
		146.76	0.4038	6.01	0.002910
Series 2		151.80	0.4210	6.53	0.003392
		156.80	0.4376	7.04	0.004116
333.09	0.8328	161.78	0.4358	7.64	0.004531
		166.75	0.4696	8.29	0.005067
Series 3		171.73	0.4850	9.06	0.005869
		176.76	0.5002	9.90	0.006513
343.77	0.8466			10.93	0.007006
347.09	0.8518	Series 8		12.12	0.007385
353.07	0.8598			13.42	0.007600
359.02	0.8678	181.44	0.5140	14.88	0.007753
364.97	0.8752	186.65	0.5291	16.51	0.007790
370.99	0.8833	192.03	0.5442	18.19	0.007949
376.97	0.8906	197.33	0.5586	20.04	0.008300
382.42	0.8965	202.54	0.5726	22.05	0.008850
387.39	0.9017	207.79	0.5859	24.18	0.009742
		213.06	0.5995	26.59	0.01124
Series 4		218.26	0.6125	29.33	0.01355
		223.40	0.6248	32.29	0.01700
53.01	0.06168	228.58	0.6371	35.67	0.02202
57.86	0.07613	233.80	0.6493	39.40	0.02861
62.33	0.09006	238.96	0.6608	43.23	0.03657
67.05	0.1058	244.06	0.6724	47.79	0.04714
71.88	0.1228			52.98	0.06150
76.90	0.1414	Series 9		58.18	0.07701
Series 5		240.02	0.6629		
		245.30	0.6751		
81.91	0.1604	250.56	0.6868		
86.89	0.1796	255.87	0.6976		
92.00	0.1993	261.33	0.7084		
97.10	0.2192	266.84	0.7196		
102.23	0.2390	272.29	0.7298		
107.18	0.2585	277.70	0.7404		
112.00	0.2769	283.07	0.7498		
116.91	0.2956				

Thermodynamic functions

The thermodynamic properties C_P°, $S_T^\circ - S_0^\circ$, $(H_T^\circ - H_0^\circ)/T$, and $-(G_T^\circ - H_0^\circ)/T$ are listed at integral temperatures from 0 to 380 K for magnesio-anthophyllite [$Mg_{6.3}Fe_{0.7}Si_8O_{22}(OH)_2$ and $Mg_7Si_8O_{22}(OH)_2$], diopside, bronzite ($Mg_{0.85}Fe_{0.15}SiO_3$), synthetic enstatite ($MgSiO_3$), and wollastonite in Tables 8 through 13, respectively.

The methods described by Westrum et al. (1968) were utilized to smooth the experimental data. The C_P° data were extrapolated from the lowest measured temperature to zero Kelvin on a plot of C_P°/T versus T^2. For diopside and wollastonite, which exhibited small anomalies in C_P°/T versus T^2 because of trace quantities of Fe^{2+} in their structure, the data were extrapolated graphically to zero Kelvin from a temperature above the anomaly. Smooth C_P° values for diopside and wollastonite between zero and approximately 15 K were obtained from this extrapolation. This procedure resulted in minor changes to the molar C_P° values in this temperature range, and negligible differences to the integrated thermodynamic properties (i.e., $S_T^\circ - S_0^\circ$). Our procedure for correcting the diopside measurements for the Schottky effect caused by the Fe^{2+} impurity can be readily justified by comparing the heat capacities from the linear extrapolation with: (1) the heat capacity measurements of Leadbetter et al. (1977) between 1.5 and 25 K on synthetic diopside, and (2) heat capacities calculated from the Debye model using a value for Θ_D of 668 K obtained from the elastic constant data of Levien et al. (1979) using the method of Robie and Edwards (1966). For magnesio-anthophyllite corrected to a pure Mg composition, C_P° was

Table 6. Low-temperature, experimental specific heats of synthetic enstatite. (Sample mass was 23.287 g (in vacuo). Data for synthetic enstatite consist of 109 measurements between 5.2 and 385.3 K.)

Temp. K	Specific heat J/(g·K)	Temp. K	Specific heat J/(g·K)	Temp. K	Specific heat J/(g·K)
Series 1		Series 5		Series 11	
318.87	0.8521	156.27	0.4506	12.75	0.000548
324.41	0.8613	161.09	0.4674	14.09	0.000798
330.33	0.8706	165.96	0.4839	15.30	0.001000
336.31	0.8801	170.83	0.5004	16.69	0.001337
342.44	0.8888	175.70	0.5163	18.27	0.001778
		180.59	0.5324	19.92	0.002447
Series 2		185.49	0.5474	21.71	0.003332
		190.41	0.5624	23.62	0.004365
348.60	0.8982	195.36	0.5771	25.77	0.005815
354.80	0.9067	200.32	0.5914	28.11	0.007649
360.97	0.9156	205.31	0.6055	30.69	0.01036
367.09	0.9242	210.23	0.6193	33.58	0.01407
373.18	0.9323	215.18	0.6324	36.79	0.01898
379.24	0.9401			39.89	0.02443
385.26	0.9463	Series 6		43.34	0.03143
				47.82	0.04138
Series 3		219.99	0.6454	52.66	0.05462
		225.00	0.6589	57.59	0.06933
52.79	0.05537	230.08	0.6714		
57.69	0.07002	235.11	0.6839	Series 12	
62.06	0.08392	240.08	0.6965		
66.69	0.09953			306.80	0.8323
71.46	0.1167	Series 7		311.94	0.8408
76.35	0.1354			317.00	0.8493
81.40	0.1554	245.01	0.7081	322.02	0.8574
86.50	0.1760	249.98	0.7196		
91.56	0.1968	254.99	0.7306	Series 13	
96.51	0.2170	259.96	0.7413		
101.29	0.2365	264.89	0.7519	5.24	0.000001
106.32	0.2570			5.91	0.000024
111.57	0.2785	Series 8		6.47	0.000079
116.70	0.2995			7.05	0.000079
		269.81	0.7614	7.89	0.000107
Series 4		274.72	0.7727	8.85	0.000224
		279.71	0.7826	9.72	0.000298
121.71	0.3200	284.66	0.7923	10.56	0.000322
126.56	0.3391	289.66	0.8030	11.48	0.000469
131.37	0.3580	294.72	0.8115	12.46	0.000582
136.34	0.3773	299.74	0.8195	13.54	0.000719
141.49	0.3968	304.73	0.8293	14.74	0.000910
146.61	0.4159	309.78	0.8375	16.08	0.001208
151.59	0.4341	314.88	0.8463	17.62	0.001601
		319.96	0.8553	19.26	0.002240
		325.00	0.8627	21.07	0.003042
		330.01	0.8705	23.07	0.004063
				25.27	0.005493

Table 7. Low-temperature, experimental specific heats of wollastonite. (Sample mass was 29.231 g (in vacuo). Data for wollastonite consist of 94 measurements between 6.3 and 386.2 K.)

Temp.	Specific Heat	Temp.	Specific Heat	Temp.	Specific Heat
K	J/(g·K)	K	J/(g·K)	K	J/(g·K)
Series 3		Series 7		Series 11	
298.81	0.7423	130.73	0.3862	271.47	0.7105
303.86	0.7494	135.64	0.4018	276.50	0.7115
309.81	0.7572	140.56	0.4169	281.54	0.7182
315.72	0.7648	145.56	0.4318	286.54	0.7259
321.68	0.7720	150.54	0.4462	291.51	0.7338
327.69	0.7795	155.51	0.4602	296.54	0.7397
333.66	0.7866	160.48	0.4739	301.62	0.7473
		165.45	0.4874	306.67	0.7537
Series 4		170.51	0.5006	311.70	0.7600
339.66	0.7934	Series 8		Series 12	
345.79	0.8002				
351.88	0.8070	175.19	0.5123	6.27	0.000074
357.93	0.8140	180.15	0.5247	7.47	0.000240
363.95	0.8197	185.16	0.5367	8.33	0.000281
369.94	0.8255	190.20	0.5486	9.01	0.000503
375.90	0.8317	195.15	0.5598	9.64	0.000481
381.83	0.8370	200.14	0.5709	10.27	0.000692
386.16	0.8413	205.16	0.5817	10.99	0.000675
		210.11	0.5916	11.85	0.000851
Series 5		215.10	0.6018	12.81	0.001104
				13.88	0.001432
52.83	0.09422	Series 9		15.05	0.001895
57.01	0.1102			16.54	0.002596
61.49	0.1274	222.57	0.6172	18.17	0.003712
66.30	0.1462	226.55	0.6249	19.78	0.005178
71.18	0.1656	231.68	0.6347	21.66	0.007197
76.06	0.1852	236.77	0.6445	23.77	0.01003
80.95	0.2056	241.74	0.6538	26.15	0.01389
85.90	0.2254	246.67	0.6625	28.78	0.01897
90.82	0.2445			31.67	0.02560
95.64	0.2626	Series 10		34.95	0.03426
100.51	0.2810			38.60	0.04486
105.51	0.2994	251.58	0.6700	42.66	0.05768
		256.62	0.6791	47.35	0.07352
Series 6		261.63	0.6886	52.38	0.09205
		266.60	0.6973	57.40	0.1112
110.49	0.3172				
115.59	0.3353				
120.93	0.3539				
126.09	0.3709				

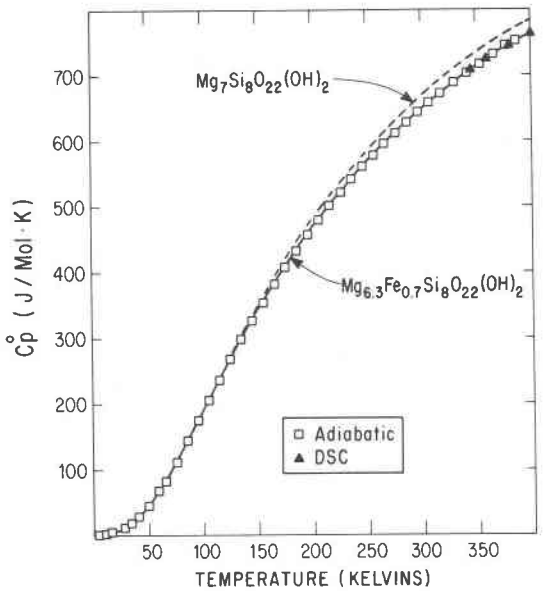

Fig. 1. Experimental molar heat capacity of natural anthophyllite [$Mg_{6.3}Fe_{0.7}Si_8O_{22}(OH)_2$]. The open squares and solid triangles are experimental data for the Mg/Fe magnesio-anthophyllite determined by adiabatic calorimetry (this study) and DSC analysis (Krupka et al., 1985), respectively. The solid line is a least-squares fit to the data. The dashed line is a least-squares fit to the data corrected to the pure Mg composition $Mg_7Si_8O_{22}(OH)_2$.

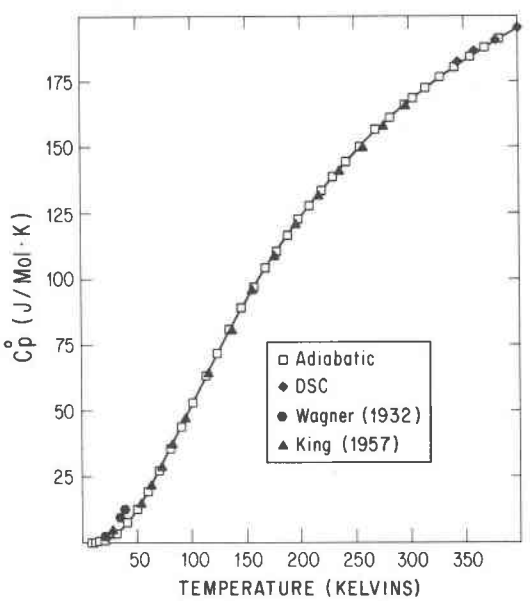

Fig. 2. Experimental molar heat capacity of diopside. The open squares and solid diamonds are data determined by adiabatic calorimetry (this study) and DSC analysis (Krupka et al., 1985), respectively. The solid hexagons and solid triangles are the low-temperature C_P° data of Wagner (1932) and King (1957), respectively. The solid line is a least-squares fit to the experimental data from this study.

extrapolated to zero Kelvin according to the principle of corresponding states (Lewis and Randall, 1961; McQuarrie, 1973) with respect to tremolite. That is, the ratio of the low-temperature C_P° per gram of tremolite (Robie and Stout, 1963) to the C_P° per gram of pure magnesio-anthophyllite was used for a smooth extrapolation to zero Kelvin.

The molar C_P° data were smoothed graphically between 0 and approximately 20 K, and analytically from 20 to 380 K by least-squares fits to orthogonal polynomials (Justice 1969). Values of $S_T^\circ - S_0^\circ$, $(H_T^\circ - H_0^\circ)/T$, and $-(G_T^\circ - H_0^\circ)/T$ were obtained by integrating the smoothed C_P° functions. The smoothed C_P° values and integrated thermodynamic properties for the Fe-bearing magnesio-anthophyllite (Table 8) and for bronzite (Table 11) retain the heat capacity contributions resulting from Fe^{2+} impurities. The entropy change $S_{298}^\circ - S_0^\circ$, in J/(mol·K), is 538.9 ± 2.7 for Mg/Fe-anthophyllite [$Mg_{6.3}Fe_{0.7}Si_8O_{22}(OH)_2$],

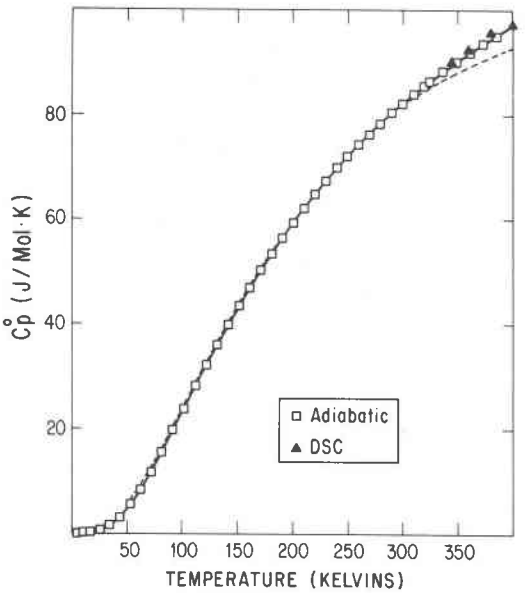

Fig. 3. Experimental molar heat capacity of synthetic enstatite $MgSiO_3$. The open squares and solid triangles are experimental data determined by adiabatic calorimetry (this study) and DSC analysis (Krupka et al., 1985), respectively. The solid line is a least-squares fit to the experimental data. The dashed line represents the C_P° function of clinoenstatite given by Kelley (1943).

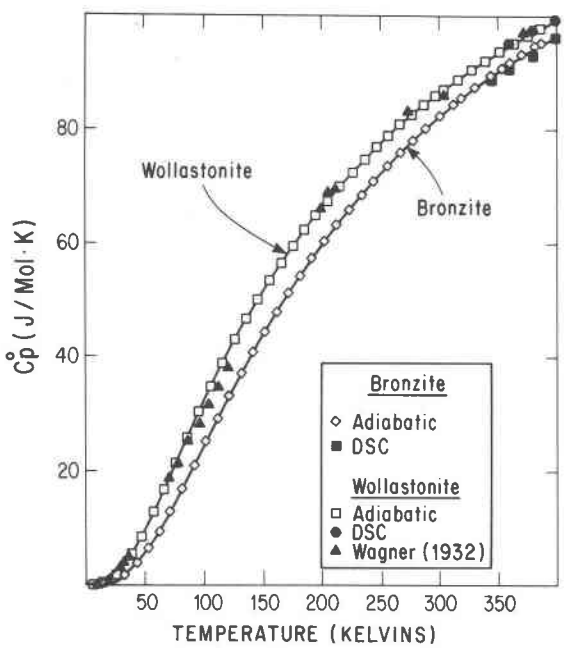

Fig. 4. Experimental molar heat capacity of bronzite ($Mg_{0.85}Fe_{0.15}SiO_3$) and wollastonite. The open diamonds and open squares are data determined by adiabatic calorimetry (this study) for bronzite and wollastonite, respectively. The solid squares and solid hexagons are data determined by DSC analysis (Krupka et al., 1985) for bronzite and wollastonite, respectively. The solid triangles are the low-temperature data of Wagner (1932) for wollastonite. The solid curves are least-squares fits to the experimental data of this study.

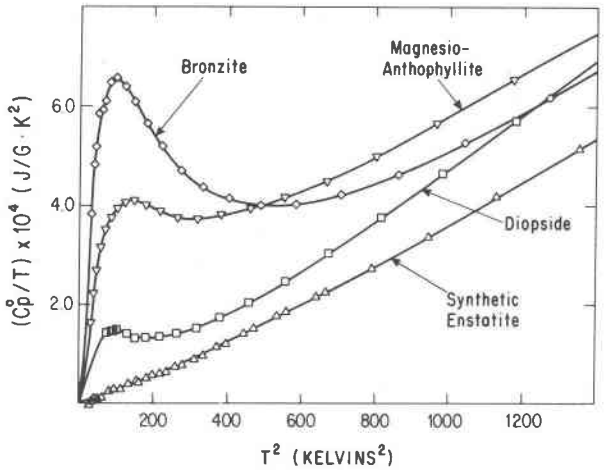

Fig. 5. Plot of C_P°/T versus T^2 showing the Schottky C_P° anomalies at low temperature for bronzite ($Mg_{0.85}Fe_{0.15}SiO_3$), magnesio-anthophyllite ($Mg_{6.3}Fe_{0.7}Si_8O_{22}(OH)_2$), and diopside. The lowest curve and data are for pure synthetic enstatite.

537.0 ± 2.7 for magnesio-anthophyllite [$Mg_7Si_8O_{22}(OH)_2$], 142.7 ± 0.2 for diopside, 69.04 ± 0.10 for bronzite ($Mg_{0.85}Fe_{0.15}SiO_3$), 66.27 ± 0.10 for synthetic enstatite ($MgSiO_3$), and 81.69 ± 0.12 for wollastonite. The larger uncertainties for the two values of magnesio-anthophyllite reflect the impurity corrections applied to the experimental C_P° data for anthophyllite.

The entropy at 298.15 K for the Fe-bearing magnesio-anthophyllite does not include a term for the configurational entropy, S_{cf}°, that could arise from the random distribution of Fe and Mg on the M sites in the amphibole structure (e.g., Ulbrich and Waldbaum, 1976). The configurational entropy was neglected for this anthophyllite sample because the cation distribution is not known for this particular sample and because cations may be partially ordered on the M sites (Finger, 1970).

Similarly, a value of S_{cf}° was not included in the tabulated results for bronzite ($Mg_{0.85}Fe_{0.15}SiO_3$) because the Mg–Fe distribution is not known for this particular sample. If the Mg and Fe were totally disordered and the two sites were treated as equivalent, this Mg–Fe distribution would result in a maximum value of S_{cf}° equal to 3.5 J/(mol·K) [i.e., R (0.85 ln 0.85 + 0.15 ln 0.15) (Ulbrich and Walbaum, 1976).]

Comparison with previous studies

Values given by King (1957) and Wagner (1932) for the low-temperature heat capacity of diopside are shown in Figure 2 for comparison with the smoothed C_P° values determined in this study. Data of the present study are in good agreement with the C_P° values of King (1957) but differ significantly from those of Wagner (1932). King's C_P° data are greater than the values from this study by 1.5% at 53.8 K to 0.10% at 72.9 K. At temperatures between 77.5 and 296.0 K, King's values are slightly lower than the new

Table 8. Low-temperature molar thermodynamic properties of magnesio-anthophyllite, $Mg_{6.3}Fe_{0.7}Si_8O_{22}(OH)_2$. (Formula weight = 802.900 g/mol)

Temp.	Heat capacity	Entropy	Enthalpy function	Gibbs energy function
T	C_P^o	$(S_T^o-S_0^o)$	$(H_T^o-H_0^o)/T$	$-(G_T^o-H_0^o)/T$
Kelvin		J/(mol•K)		
5	0.548	0.166	0.124	0.041
10	3.162	1.365	1.005	0.360
15	4.641	2.974	2.009	0.965
20	6.132	4.485	2.829	1.656
25	8.745	6.111	3.730	2.381
30	12.90	8.044	4.886	3.158
35	18.94	10.46	6.440	4.023
40	26.36	13.46	8.453	5.009
45	35.30	17.07	10.92	6.143
50	45.54	21.31	13.86	7.443
60	69.26	31.65	21.06	10.58
70	96.42	44.32	29.85	14.47
80	126.1	59.11	40.01	19.11
90	157.2	75.75	51.29	24.46
100	188.9	93.95	63.47	30.49
110	220.6	113.5	76.32	37.13
120	251.9	134.0	89.65	44.34
130	282.5	155.4	103.3	52.06
140	312.3	177.4	117.2	60.22
150	341.1	199.9	131.2	68.78
160	368.7	222.8	145.2	77.69
170	395.1	246.0	159.1	86.91
180	420.4	269.3	172.9	96.40
190	444.6	292.7	186.6	106.1
200	467.7	316.1	200.1	116.0
210	489.9	339.4	213.3	126.1
220	511.1	362.7	226.4	136.3
230	531.3	385.9	239.2	146.7
240	550.5	408.9	251.8	157.1
250	568.9	431.8	264.1	167.7
260	586.5	454.4	276.2	178.3
270	603.5	476.9	288.0	188.9
280	619.8	499.1	299.5	199.6
290	635.3	521.1	310.9	210.3
300	649.8	542.9	321.9	221.0
310	663.6	564.5	332.7	231.7
320	676.8	585.7	343.3	242.5
330	689.7	606.8	353.6	253.2
340	702.3	627.5	363.6	263.9
350	714.3	648.1	373.5	274.6
360	725.9	668.4	383.1	285.2
370	737.2	688.4	392.5	295.9
380	747.7	708.2	401.7	306.5
273.15	608.7	483.9	291.6	192.3
298.15	647.2	538.9	319.9	219.0

C_P^o data by 0.3%. At 298.15 K, our entropy for diopside is 0.3% less than King's value. On the other hand, Wagner's C_P^o values (20.7 – 39.3 K) are all approximately 100% greater than the values obtained in this study.

The smooth low-temperature C_P^o values for wollastonite, shown in Figure 4, are in significant disagreement with the wollastonite data of Wagner (1932). Wagner's C_P^o data at the lowest temperatures (9.8 – 35.5 K) are greater than our values by 155% at 9.8 K and 26.4% at 19.5 K. Wagner's data from 70.7 to 120.1 K are all lower than our C_P^o values by an average 6%. At the higher temperatures (199.7 – 373.2 K), the agreement is better, and Wagner's data are 1.5% greater than the C_P^o values from this study. The good agreement between our value of $S_{298}^o - S_0^o$ for wollastonite and that calculated by Kelley and King (1961) from C_P^o data of Wagner (1932) is strictly fortuitous.

Magnetic contributions to the entropy of $Mg_{0.85}Fe_{0.15}SiO_3$

The measured C_P^o of bronzite ($Mg_{0.85}Fe_{0.15}SiO_3$) at liquid-helium temperatures is significantly greater than that for synthetic enstatite. This anomalous behavior is especially apparent when the data are plotted in the form of C_P^o/T versus T^2 (Fig. 5). The larger values of C_P^o/T are

Table 9. Low-temperature molar thermodynamic properties of anthophyllite corrected to pure Mg composition, $Mg_7Si_8O_{22}(OH)_2$. (Formula weight = 780.874 g/mol)

Temp.	Heat capacity	Entropy	Enthalpy function	Gibbs energy function
T	C_P^o	$(S_T^o-S_0^o)$	$(H_T^o-H_0^o)/T$	$-(G_T^o-H_0^o)/T$
Kelvin		J/(mol•K)		
5	0.039	0.0132	0.0096	0.0036
10	0.299	0.101	0.075	0.026
15	1.020	0.338	0.253	0.085
20	2.480	0.810	0.608	0.202
25	4.998	1.610	1.213	0.397
30	8.856	2.839	2.144	0.695
35	14.49	4.600	3.479	1.121
40	21.81	6.995	5.296	1.699
45	30.58	10.05	7.596	2.451
50	40.87	13.79	10.40	3.392
60	65.00	23.31	17.43	5.882
70	92.88	35.38	26.18	9.205
80	123.5	49.76	36.40	13.35
90	155.6	66.14	47.85	18.29
100	188.5	84.24	60.27	23.97
110	221.3	103.7	73.42	30.32
120	253.6	124.4	87.09	37.30
130	285.3	145.9	101.1	44.82
140	316.0	168.2	115.4	52.83
150	345.8	191.0	129.8	61.29
160	374.3	214.3	144.2	70.12
170	401.7	237.8	158.5	79.29
180	427.8	261.5	172.7	88.75
190	452.8	285.3	186.8	98.47
200	476.8	309.1	200.7	108.4
210	499.8	333.0	214.4	118.5
220	521.8	356.7	227.9	128.8
230	542.8	380.4	241.1	139.2
240	562.7	403.9	254.1	149.8
250	581.9	427.3	266.9	160.4
260	600.3	450.5	279.3	171.1
270	618.0	473.4	291.5	181.9
280	635.0	496.2	303.5	192.7
290	651.1	518.8	315.2	203.6
300	666.2	541.1	326.7	214.5
310	680.5	563.2	337.9	225.3
320	694.2	585.0	348.8	236.2
330	707.6	606.6	359.4	247.1
340	720.6	627.9	369.9	258.0
350	733.1	649.0	380.1	268.9
360	745.1	669.8	390.1	279.7
370	756.9	690.4	399.8	290.6
380	767.7	710.7	409.4	301.4
273.15	623.4	480.6	295.3	185.3
298.15	663.5	537.0	324.6	212.4

Table 10. Low-temperature molar thermodynamic properties of diopside, $CaMg(SiO_3)_2$. (Formula weight = 216.553 g/mol)

Temp.	Heat capacity	Entropy	Enthalpy function	Gibbs energy function
T	C_P^o	$(S_T^o-S_0^o)$	$(H_T^o-H_0^o)/T$	$-(G_T^o-H_0^o)/T$
Kelvin		J/(mol·K)		
5	0.009	0.0030	0.0022	0.0008
10	0.082	0.026	0.019	0.007
15	0.297	0.093	0.071	0.022
20	0.755	0.234	0.178	0.056
25	1.544	0.482	0.368	0.114
30	2.790	0.866	0.660	0.206
35	4.576	1.424	1.086	0.338
40	6.799	2.176	1.657	0.518
45	9.424	3.124	2.371	0.753
50	12.42	4.269	3.223	1.046
60	19.29	7.124	5.313	1.811
70	27.02	10.67	7.854	2.816
80	35.28	14.81	10.76	4.051
90	43.80	19.46	13.96	5.501
100	52.40	24.52	17.37	7.146
110	60.92	29.91	20.94	8.969
120	69.21	35.57	24.62	10.95
130	77.19	41.43	28.36	13.07
140	84.82	47.43	32.12	15.31
150	92.11	53.53	35.88	17.65
160	99.09	59.70	39.62	20.09
170	105.7	65.91	43.31	22.60
180	112.1	72.14	46.96	25.18
190	118.0	78.36	50.54	27.81
200	123.7	84.56	54.06	30.50
210	129.0	90.72	57.50	33.22
220	134.1	96.84	60.87	35.97
230	139.0	102.9	64.16	38.75
240	143.8	108.9	67.38	41.55
250	148.4	114.9	70.53	44.36
260	152.7	120.8	73.61	47.19
270	156.7	126.6	76.62	50.02
280	160.4	132.4	79.54	52.86
290	164.0	138.1	82.40	55.70
300	167.4	143.7	85.17	58.54
310	170.7	149.3	87.88	61.38
320	174.0	154.7	90.52	64.21
330	177.1	160.1	93.10	67.04
340	179.9	165.5	95.61	69.86
350	182.7	170.7	98.06	72.66
360	185.5	175.9	100.4	75.46
370	188.2	181.0	102.8	78.24
380	190.7	186.1	105.1	81.01
273.15	157.9	128.5	77.55	50.92
298.15	166.8	142.7	84.66	58.02

presumably caused by the substitution of Fe^{2+} for Mg^{2+} in the bronzite, thus permitting either a Schottky-type heat capacity contribution and/or a cooperative (i.e., spin-ordering) transition (Gopal, 1966). In either case, the total magnetic entropy (S°_{Mag}) arising from the spins of the Fe^{2+} ions in the bronzite is:

$$S^\circ_{Mag} = n\,R\,\ln(2s+1),$$

where s is the spin quantum number and equal to 2 for Fe^{2+} (Gopal, 1966). Thus, S°_{Mag} for $Mg_{0.85}Fe_{0.15}SiO_3$ (where n = 0.15) is 2.01 J/(mol·K). The observed entropy arising from anomalous heat capacities between 5 and 30 K is approximately 1 J/(mol·K) or only 50 percent of the expected magnetic entropy.

Based on their Mössbauer studies, Shenoy et al. (1969) concluded that, for bronzite ($Fe_xMg_{1-x}SiO_3$) where $x < 0.39$, there is no magnetic ordering down to 1.7 K. Therefore, we may exclude cooperative ordering of the spins as a source of the anomalous heat capacities.

In order to test the possibility that the anomalous heat capacities are due to a Schottky effect, we have assumed that the *lattice* heat capacity of $Mg_{0.85}Fe_{0.15}SiO_3$ below approximately 20 K obeys the Debye model. The elastic constant values of Frisillo and Barsch (1972) for a bronzite

Table 11. Low-temperature molar thermodynamic properties of bronzite, $Mg_{0.85}Fe_{0.15}SiO_3$. (Formula weight = 105.120 g/mol)

Temp.	Heat capacity	Entropy	Enthalpy function	Gibbs energy function
T	C_P^o	$(S_T^o-S_0^o)$	$(H_T^o-H_0^o)/T$	$-(G_T^o-H_0^o)/T$
Kelvin		J/(mol·K)		
5	0.146	0.035	0.027	0.008
10	0.694	0.329	0.241	0.088
15	0.817	0.643	0.420	0.223
20	0.874	0.883	0.524	0.359
25	1.075	1.096	0.611	0.485
30	1.503	1.327	0.721	0.606
35	2.213	1.608	0.879	0.729
40	3.137	1.960	1.101	0.859
45	4.285	2.394	1.389	1.005
50	5.617	2.913	1.744	1.169
60	8.726	4.204	2.641	1.563
70	12.29	5.812	3.760	2.052
80	16.16	7.702	5.065	2.637
90	20.21	9.838	6.522	3.316
100	24.34	12.18	8.097	4.084
110	28.44	14.69	9.760	4.933
120	32.46	17.34	11.49	5.856
130	36.38	20.10	13.25	6.845
140	40.17	22.93	15.04	7.892
150	43.82	25.83	16.84	8.991
160	47.32	28.77	18.63	10.14
170	50.66	31.74	20.42	11.32
180	53.84	34.72	22.19	12.54
190	56.86	37.72	23.93	13.78
200	59.74	40.71	25.65	15.05
210	62.48	43.69	27.34	16.35
220	65.11	46.66	29.00	17.66
230	67.63	49.61	30.62	18.98
240	70.04	52.54	32.22	20.32
250	72.35	55.44	33.78	21.67
260	74.54	58.32	35.30	23.02
270	76.63	61.18	36.80	24.38
280	78.61	64.00	38.25	25.75
290	80.50	66.79	39.68	27.11
300	82.32	69.55	41.07	28.48
310	84.08	72.28	42.43	29.85
320	85.78	74.98	43.76	31.22
330	87.39	77.64	45.05	32.58
340	88.90	80.27	46.32	33.95
350	90.34	82.87	47.56	35.31
360	91.75	85.43	48.77	36.67
370	93.14	87.97	49.95	38.02
380	94.40	90.47	51.10	39.37
273.15	77.26	62.07	37.26	24.81
298.15	81.99	69.04	40.81	28.23

Table 12. Low-temperature molar thermodynamic properties of synthetic enstatite, $MgSiO_3$. (Formula weight = 100.389 g/mol)

Temp.	Heat capacity	Entropy	Enthalpy function	Gibbs energy function
T	C_P^o	$(S_T^o-S_0^o)$	$(H_T^o-H_0^o)/T$	$-(G_T^o-H_0^o)/T$
Kelvin		J/(mol·K)		
5	0.004	0.0012	0.0009	0.0003
10	0.029	0.0096	0.0072	0.0024
15	0.095	0.032	0.024	0.008
20	0.252	0.078	0.059	0.019
25	0.526	0.161	0.123	0.038
30	0.958	0.292	0.223	0.069
35	1.617	0.487	0.373	0.114
40	2.471	0.756	0.579	0.177
45	3.524	1.106	0.846	0.260
50	4.764	1.540	1.175	0.366
60	7.729	2.662	2.012	0.650
70	11.21	4.109	3.072	1.037
80	15.04	5.853	4.325	1.527
90	19.08	7.856	5.739	2.117
100	23.21	10.08	7.280	2.800
110	27.34	12.49	8.916	3.570
120	31.41	15.04	10.62	4.419
130	35.40	17.71	12.38	5.338
140	39.26	20.48	14.16	6.320
150	42.99	23.32	15.96	7.359
160	46.56	26.21	17.76	8.446
170	49.97	29.13	19.55	9.577
180	53.22	32.08	21.34	10.74
190	56.32	35.04	23.10	11.95
200	59.28	38.01	24.83	13.17
210	62.11	40.97	26.54	14.43
220	64.82	43.92	28.22	15.70
230	67.40	46.86	29.87	16.99
240	69.86	49.78	31.48	18.30
250	72.21	52.68	33.06	19.61
260	74.44	55.55	34.61	20.94
270	76.58	58.40	36.13	22.28
280	78.62	61.23	37.61	23.62
290	80.56	64.02	39.06	24.96
300	82.39	66.78	40.47	26.31
310	84.12	69.51	41.85	27.66
320	85.77	72.21	43.20	29.01
330	87.36	74.87	44.51	30.36
340	88.89	77.50	45.80	31.71
350	90.35	80.10	47.05	33.05
360	91.78	82.67	48.27	34.40
370	93.17	85.20	49.47	35.73
380	94.46	87.70	50.63	37.07
273.15	77.24	59.30	36.60	22.70
298.15	82.06	66.27	40.21	26.06

of composition $Mg_{0.8}Fe_{0.2}SiO_3$ were used to calculate a Debye temperature of 710 K with the methods described by Robie and Edwards (1966). We used this Debye temperature to calculate the lattice heat capacity, which was then subtracted from the measured heat capacity to obtain that part arising from the Schottky contribution. The simplest model that provides a reasonable fit (Fig. 6) to the residual heat capacities was obtained with a two-level model having a doubly degenerate ground level and a triplet at 22.5 cm^{-1}. The agreement with the Schottky model does not mean that these are necessarily the correct energy levels. It is likely, however, that the two levels are not totally degenerate. In this case, an additional heat capacity maximum would be expected at a temperature below 1.7 K, arising from the splitting of the ground-state doublet. Our heat capacity extrapolation to zero Kelvin did not include this contribution to the entropy. This additional entropy would be ≤ 0.86 J/(mol · K) (i.e., 0.15 R (ln 2)).

Moreover, to obtain the entropy value for use in equilibrium calculations involving $Mg_{0.85}Fe_{0.15}SiO_3$, one must also add the configurational entropy (discussed previously) arising from the substitution of Fe^{2+} for Mg^{2+}.

Table 13. Low-temperature molar thermodynamic properties of wollastonite, $CaSiO_3$. (Formula weight = 116.164 g/mol)

Temp.	Heat capacity	Entropy	Enthalpy function	Gibbs energy function
T	C_P^o	$(S_T^o-S_0^o)$	$(H_T^o-H_0^o)/T$	$-(G_T^o-H_0^o)/T$
Kelvin		J/(mol·K)		
5	0.006	0.0021	0.0016	0.0005
10	0.057	0.018	0.014	0.004
15	0.217	0.066	0.050	0.016
20	0.622	0.175	0.135	0.040
25	1.389	0.389	0.302	0.087
30	2.522	0.737	0.573	0.164
35	4.006	1.233	0.954	0.280
40	5.713	1.877	1.439	0.438
45	7.625	2.659	2.019	0.640
50	9.693	3.568	2.682	0.886
60	14.14	5.723	4.216	1.507
70	18.78	8.249	5.963	2.286
80	23.43	11.06	7.857	3.205
90	28.01	14.09	9.843	4.244
100	32.44	17.27	11.88	5.386
110	37.60	20.56	13.95	6.616
120	40.76	23.93	16.01	7.918
130	44.60	27.35	18.07	9.281
140	48.22	30.79	20.09	10.69
150	51.65	34.23	22.08	12.15
160	54.90	37.67	24.03	13.64
170	57.99	41.09	25.94	15.15
180	60.91	44.49	27.80	16.69
190	63.67	47.86	29.62	18.24
200	66.26	51.19	31.39	19.80
210	68.71	54.48	33.11	21.38
220	71.05	57.73	34.78	22.95
230	73.31	60.94	36.40	24.54
240	75.52	64.11	37.99	26.12
250	77.66	67.23	39.53	27.70
260	79.70	70.32	41.04	29.28
270	81.60	73.36	42.51	30.86
280	83.34	76.36	43.93	32.43
290	84.95	79.32	45.32	34.00
300	86.47	82.22	46.67	35.56
310	87.95	85.08	47.98	37.11
320	89.42	87.90	49.25	38.65
330	90.85	90.67	50.49	40.18
340	92.21	93.40	51.69	41.71
350	93.49	96.10	52.87	43.23
360	94.73	98.75	54.02	44.73
370	95.93	101.36	55.13	46.23
380	97.02	103.93	56.22	47.71
273.15	82.17	74.31	42.96	31.35
298.15	86.19	81.69	46.42	35.27

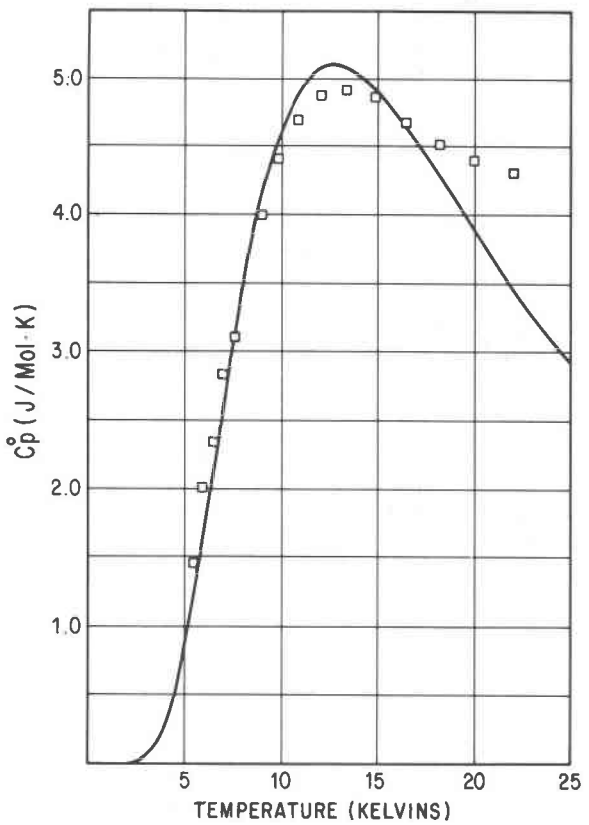

Fig. 6. Schottky heat capacities for bronzite ($Mg_{0.85}Fe_{0.15}SiO_3$). The open squares are data determined in this study by adiabatic calorimetry. The solid line is calculated from equation 4.25 in Gopal (1966) with $g_1/g_0 = 1.5$ and $\delta = 22.5$ cm^{-1}.

Acknowledgments

This paper is partly based on K. M. Krupka's Ph.D. research at The Pennsylvania State University. Profs. Bernard W. Evans and Peter Misch at the University of Washington kindly provided the anthophyllite sample, and J. Stephen Huebner of the U.S. Geological Survey, Reston, Va., provided the bronzite sample. The authors are particularly grateful to Dr. David Veblen, who, while at Arizona State University, inspected a section of the anthophyllite sample for the presence of hydrous pyribole structures. We also thank Howard T. Evans, Jr., of the U.S. Geological Survey, J. Stephen Huebner, Lowell B. Wiggins of IBM Corporation, and analysts of the U.S. Geological Survey, Reston, Va., for their invaluable assistance in the characterization and chemical analysis of our samples. We are also grateful to John L. Haas, Jr., Henry T. Hazelton, Jr., Susan W. Kieffer, and Donald E. Voight, all of the U.S. Geological Survey, and Bruce D. Velde at Ecole Normale Supérior, Paris, France, for critically reviewing the manuscript and for their helpful comments. This work was supported by the U.S. Geological Survey and by grants EAR 76-84199 and EAR 79-08244 from the Earth Sciences Division of the National Science Foundation to D. M. Kerrick. We also thank the Battelle, Pacific Northwest Laboratory for providing funds for the preparation of this manuscript.

References

Appleman, D. E. and Evans, T. H., Jr. (1963) Job 9214: Indexing and least-squares refinement of powder diffraction data. National Technical Information Services, U.S. Dept. Commerce, Springfield, Virginia, Document PB-216 188.

Bearth, P. (1970) Zur Eklogitbildung in den Westalpen. Fortschritte der Mineralogie, 47, 27–33.

Bence, A. E. and Albee, A. L. (1968) Empirical correction factors for the electron microprobe analysis of silicates and oxides. Journal of Geology, 76, 382–403.

Bennington, K. O., Ferrante, M. J., and Stuve, J. M. (1978) Thermodynamic data on the amphibole asbestos minerals amosite and crocidolite. U.S. Bureau Mines Report of Investigation 8265.

Borg, I. Y. and Smith, D. K. (1969) Calculated X-ray powder patterns for silicate minerals. Geological Society of America Memoir 122.

Buerger, M. J. and Prewitt, C. T. (1961) The crystal structures of wollastonite and pectolite. Proceedings of the National Academy of Sciences, 47, 1884–1888.

Chernosky, J. V., Jr. and Autio, L. K. (1979) The stability of anthophyllite in the presence of quartz. American Mineralogist, 64, 294–303.

Commission on Atomic Weights (1976) Atomic weights of the elements 1975. Pure and Applied Chemistry, 47, 75–94.

Finger, L. W. (1970) Refinement of the crystal structure of an anthophyllite. Carnegie Institute of Washington Year Book, 68, 283–288.

Frisillo, A. L. and Barsch, G. R. (1972) Measurement of single-crystal elastic constants of bronzite as a function of pressure and temperature. Journal of Geophysical Research, 77, 6360–6384.

Furukawa, G. T., Douglas, T. B., McCoskey, R. E., and Ginnings, D. C. (1956) Thermal properties of aluminum oxide from 0 to 1200°K. National Bureau of Standards Journal of Research, 57, 67–82.

Gopal, E. S. R. (1966) Specific Heats at Low Temperatures. Plenum Press, New York.

Gronvold, F. and Westrum, E. F., Jr. (1959) α-Ferric oxide: Low temperature heat capacity and thermodynamic functions. Journal of the American Chemical Society, 81, 1780–1783.

Gronvold, F., Westrum, E. F., Jr., and Chou, C. (1959) Heat capacities and thermodynamic properties of the pyrrhotites FeS and $Fe_{0.877}S$ from 5 to 350 K. Journal of Chemical Physics, 30, 528–531.

Hellman, M. S. (1971) X-ray diffractometer data reduction program. U.S. Geological Survey, Computer Contribution No. 9.

Huebner, J. S., Duba, A., and Wiggings, L. B. (1979) Electrical conductivity of pyroxene which contains trivalent cations: Laboratory measurements and the lunar temperature profile. Journal of Geophysical Research, 84, 4652–4656.

Ito, J. (1975) High temperature solvent growth of orthoenstatite, $MgSiO_3$, in air. Geophysical Research Letters, 2, 533–536.

Justice, B. H. (1969) Thermal data fitting with orthogonal functions and combined table generation. U.S. Atomic Energy Commission Report C00-1149-143.

Kelley, K. K. (1943) Specific heats at low temperature of magnesium orthosilicate and magnesium metasilicate. Journal of the American Chemical Society, 65, 339–341.

Kelley, K. K., and King, E. G. (1961) Contributions to the data on theoretical metallurgy. XIV. Entropies of the elements and inorganic compounds. U.S. Bureau of Mines Bulletin 592.

King, E. G. (1957) Low temperature heat capacities and entropies

at 298.15 K of some crystalline silicates containing calcium. Journal of the American Chemical Society, 79, 5437–5438.

Krupka, K. M. (1984) Thermodynamic Analysis of Some Equilibria in the System MgO–SiO_2–H_2O. Ph.D. Thesis, The Pennsylvania State University, University Park.

Krupka, K. M., Hemingway, B. S., Robie, R. A., and Kerrick, D. M. (1985) High-temperature heat capacities and derived thermodynamic properties of anthophyllite, diopside, dolomite, enstatite, bronzite, talc, tremolite, and wollastonite. American Mineralogist, 70, 261–271.

Leadbetter, A. J., Jeapes, A. P. Waterfield, C. G., and Wycherly, K. E. (1977) The low temperature heat capacity of some glass ceramics. Chemical Physics Letters, 52, 469–472.

Levien, L., Weidner, D. J., and Prewitt, C. T. (1979) Elasticity of diopside. Physics and Chemistry of Minerals, 4, 105–113.

Lewis, G. N., and Randall, M. (1961) Thermodynamics. Second Edition, revised by K. S. Pitzer and L. Brewer. McGraw-Hill, New York.

McQuarrie, D. A. (1973) Statistical Thermodynamics. Harper and Row, New York.

Robie, R. A., and Edwards, J. L. (1966) Some Debye temperatures from single-crystal elastic constant data. Journal of Applied Physics, 37, 2659–2663.

Robie, R. A. and Hemingway, B. S. (1972) Calorimeters for heat of solution and low-temperature heat capacity measurements. U.S. Geological Survey Professional Paper 755.

Robie, R. A. and Stout, J. W. (1963) Heat capacity from 12 to 305° K and entropy of talc and tremolite. Journal of Physical Chemistry, 67, 2252–2256.

Robie, R. A., Hemingway, B. S., and Wilson, W. H. (1976) The heat capacities of Calorimetry Conference copper and of muscovite $KAl_2(AlSi_3)O_{10}(OH)_2$, pyrophyllite $Al_2Si_4O_{10}(OH)_2$, and illite $K_3(Al_7Mg)(Si_{14}Al_2)O_{40}(OH)_8$ between 15 and 375 K and their standard entropies at 298.15 K. U.S. Geological Survey Journal of Research, 4(6) 631–644.

Robie, R. A., Hemingway, B. S., and Wilson, W. H. (1978) Low-temperature heat capacities and entropies of $KAlSi_3O_8$, $NaAlSi_3O_8$, and $CaAl_2Si_2O_8$ glasses and of anorthite. American Mineralogist, 63, 110–123.

Shapiro, Leonard, (1975) Rapid analysis of silicate, carbonate, and phosphate rocks—revised edition. U.S. Geological Survey Bulletin 1401.

Shenoy, G. K., Kalvius, G. Michael, and Hafner, S. S. (1969) Magnetic behavior of the iron silicate–magnesium silicate orthopyroxene system from N.G.R. [Nuclear γ-ray resonance] in iron-57. Journal of Applied Physics, 40, 1314–1316.

Slaughter, J., Kerrick, D. M., and Wall, V. J. (1975) Experimental and thermodynamic study of equilibria in the system CaO–MgO–SiO_2–H_2O–CO_2. American Journal of Science, 275, 143–162.

Smith, J. V. (1969) Crystal structure and stability of the $MgSiO_3$ polymorphs; physical properties and phase relations of Mg,Fe pyroxenes. In J. J. Papike, Ed., Pyroxenes and Amphiboles: Crystal Chemistry and Phase Petrology, p. 3–29, Mineralogical Society of America, Special Paper No. 2.

Ulbrich, H. H. and Waldbaum, D. R. (1976) Structural and other contributions to the third-law entropies of silicates. Geochimica et Cosmochimica Acta, 40, 1–24.

Veblen, D. R. and Burnham, C. W. (1978a) New biopyriboles from Chester, Vermont: I. Descriptive mineralogy. American Mineralogist, 63, 1000–1009.

Veblen, D. R. and Burnham, C. W. (1978b) New biopyriboles from Chester, Vermont: II. The crystal chemistry of jimthompsonite, clinojimthompsonite, and chesterite, and the amphibole-mica reaction. American Mineralogist, 63, 1053–1073.

Velblen, D. R. and Buseck, P. R. (1979) Serpentine minerals: intergrowths and new combination structures. Science, 206, 1398–1400.

Veblen, D. R., Buseck, P. R., and Burnham, C. W. (1977) Asbestiform chain silicates: New minerals and structural groups. Science, 198, 359–365.

Wagner, V. H. (1932) Zur Thermochemie der Metasilikate des Calciums und Magnesiums unds des Diopsids. Zeitschrift für Anorganische und Allgemeine Chemie, 208, 1–22.

Westrum, E. F., Jr., Furukawa, G. T., and McCullough, J. P. (1968) Adiabatic low-temperature calorimetry. In J. P. McCullough and D. W. Scott, Eds., Experimental Thermodynamics, Vol. 1, Calorimetry of Nonreacting Systems, p. 133–214. New York, Plenum Press.

Manuscript received, December 7, 1983;
accepted for publication, November 19, 1984.